ry", McGraw-Hill, New York, N.Y., 1970.
(36) S. F. Nelsen and J. P. Gillespie, *J. Am. Chem. Soc.*, **95**, 2940 (1973).
(37) H. A. Jahn and E. Teller, *Proc. R. Soc. London, Ser. A*, **161**, 220 (1937); for an example of a species having a singlet ground state because of this effect, see H. E. Zimmerman and J. R. Dodd, *J. Am. Chem. Soc.*, **92**, 6507 (1970).
(38) (a) M. Glasbeek, J. D. W. Van Vorrst, and G. H. Hoijtink, *J. Chem. Phys.*, **45** 1852 (1966); (b) see discussion in ref 27, p 244–245.
(39) A. J. Wenham and J. S. Whitehurst, *J. Chem. Soc.*, 3857 (1956).
(40) E. E. van Tamelen, R. S. Dewey, and R. J. Timmons, *J. Am. Chem. Soc.*, **83**, 8725 (1961).
(41) R. Breslow, H. W. Chang, R. Hill, and E. Wasserman, *J. Am. Chem. Soc.*, **89**, 1112 (1967).
(42) NOTE ADDED IN PROOF. We have recently observed the triplet state (ESV) of the parent 1,8-naphthoquinodimethane (**1**) and hope to report on it shortly.

Protonation Kinetics and Mechanism for 1,8-Dihydroxyanthraquinone and Anthraquinone Anion Radicals in Dimethylformamide Solvent

R. M. Wightman,[1a] J. R. Cockrell,[1a] Royce W. Murray,*[1a] J. N. Burnett,[1b] and S. B. Jones[1b]

Contribution from the William Rand Kenan, Jr., Laboratories of Chemistry, University of North Carolina, Chapel Hill, North Carolina 27514, and the Department of Chemistry, Davidson College, Davidson, North Carolina 28036. *Received June 7, 1975*

Abstract: Protonation of the radical anion of 1,8-dihydroxy-9,10-anthraquinone ($DAQ\cdot^-$) by benzoic acid is first order in acid, second in radical anion, and involves formation of an acid–radical heteroconjugate dimer in an unfavorable, labile equilibrium, followed by rate-limiting electron-transfer reduction of dimer by $DAQ\cdot^-$. Anthraquinone anion radical ($AQ\cdot^-$) is protonated by the Paul–Lipkin–Weissman mechanism with rate limitation shifting to the electron-transfer step at longer reaction times. Both protonation reactions are reversible with modest equilibrium constants.

Introduction

Two-electron electrochemical reductions for aromatic hydrocarbons and quinones in aprotic solvents in the presence of proton donors are classically thought to proceed by the mechanism[2,3]

$$Q + e \rightarrow Q\cdot^- \quad (1)$$

$$Q\cdot^- + HB \rightarrow QH\cdot + B^- \quad (2)$$

$$QH\cdot + e \rightarrow QH^- \quad (3)$$

$$QH^- + HB \rightarrow QH_2 + B^- \quad (4)$$

This mechanism, known as the ECE reaction sequence, was introduced by Hoijtink[4,5] for aromatic hydrocarbons and was extended to quinones by Peover.[6-8] The essential point of the ECE sequence is that the electron affinity of QH· exceeds that of Q ($E°_{QH,QH^-}$ is more positive than $E°_{Q,Q^-}$), so that reaction 3 proceeds rapidly at electrode potentials causing reaction 1 to occur.

It is now recognized that other reaction mechanisms exist which might kinetically compete with the ECE sequence to yield the same overall products. For example, rather than proceeding heterogeneously at the electrode in reaction 3, the second electron step may proceed through the radical anion

$$QH\cdot + Q\cdot^- \rightleftarrows QH^- + Q \quad (5)$$

This homogeneous electron-transfer pathway was pointed out by Feldberg,[9,10] and observations on it have been reviewed by Saveant.[11] Implicit in both views is overall rate control by reaction 2, written as irreversible and as first order in both radical anion and acid.

Another mechanistic alternative involves disproportionation of the radical anion prior to protonation.[12-14]

$$2Q\cdot^- \rightleftarrows Q + Q^{2-} \quad (6)$$

$$Q^{2-} + HB \rightarrow QH^- + B^- \quad (7)$$

$$QH^- + HB \rightarrow QH_2 + B^- \quad (8)$$

This reaction sequence is perhaps less generally plausible than reaction 5 owing to the very small equilibrium constant (K_{disp}) for reaction 6 under most electrochemical conditions.

A number of direct stop-flow kinetic investigations of protonations of aromatic hydrocarbon radical anions by weak acids in aprotic media have appeared in recent years. These studies, made from the physical organic point of view, were conducted principally in tetrahydrofuran and dimethoxyethane solvents and employed alkali metals to generate the radical anions, so that ion pairing effects were important. Sodium naphthalenide was studied by Bank,[15] who identified reaction sequence 2,5,4 as the protonation pathway. This sequence is known as the Paul–Lipkin–Weissman[16] mechanism. Szwarc[17] studied sodium perylenide protonation by water and alcohols in THF and found second-order decay of radical and the sequence 6,7,8. Anthracenide has been extensively examined by Bank,[18] Szwarc,[19] and Dye.[20] A range of protonation rates and mechanisms, including sequences 2,5,4, 6,7,8, and solvation of ion pairs by HB before electron transfer, was observed depending on solvent, acid donor, and alkali metal. The reactions observed ran to completion and were unaffected by the conjugate base of the protonating acid. While none of these investigations were conducted under conventional electrochemical conditions (more polar solvents, no alkali metal cations present), their results do emphasize the need to consider mechanistic alternatives to the ECE sequence in electrochemistry. They also show that reaction 2 cannot implicitly

be assumed to be a single or necessarily simple reaction step.

We[21] and others[22,23] have been interested in the use of conventional stop-flow techniques to assist interpretation of electrochemical reactions. We have carried out stop-flow studies of the protonation of the anion radicals of the quinones 1,8-dihydroxy-9,10-anthraquinone (DAQ) and 9,10-anthraquinone (AQ) by benzoic acid (HBz) in dimethylformamide solvent. $DAQ^{\cdot -}$ and $AQ^{\cdot -}$ were prepared by exhaustive electrolysis of quinones in 0.1 M tetrabutylammonium perchlorate supporting electrolyte. We find that protonations of $DAQ^{\cdot -}$ and AQ^{-} are reversible processes and are not adequately described by any of the prior mechanistic schemes.

Experimental Section

Chemicals. Spectrograde *N,N*-dimethylformamide solvent (MCB) was refluxed for 6 h over 4A molecular sieves (MCB), fractionally distilled under vacuum at 35 °C, and maintained under dry nitrogen during preparation of solutions. Reagent grade chemicals were 1,8-dihydroxy-9,10-anthraquinone (Aldrich), benzoic acid (Merck), 9,10-anthraquinone (local, sublimed twice in vacuo), and tetrabutylammonium perchlorate ($TBA^+ClO_4^-$) (G. F. Smith, recrystallized twice from hot ethanol and dried under vacuum at 65 °C). Tetrabutylammonium benzoate was prepared by reaction of benzoic acid and tetrabutylammonium hydroxide solutions (25% in methanol, Eastman). All kinetics solutions were thoroughly degassed with nitrogen for 30 min before use and contained 0.1 M $TBA^+ClO_4^-$ as supporting electrolyte. Quinone solutions were converted to quinone radical anion by reduction at a mercury pool cathode in a three-electrode cell. The radical anion is stable for several hours.

Spectra. Spectra of reactants and products were obtained using two techniques. In the "batch method", the radical solution is transported in a closed and thoroughly flushed system to a 1-cm cell in a Unicam SR1800 spectrophotometer. Provision is made for flow mixing with acid exterior to the spectrophotometer so that protonated product spectra could be observed.

In the second method, solutions of quinone and various quantities of acid are electrolyzed in the confines of an optically transparent thin-layer electrode[24,25] (OTTLE) placed in the spectrophotometer light beam. The OTTLE cell allows rapid exhaustive coulometry and convenient assessment of reaction product spectra. Construction details are available.[26,27]

Stop-Flow Experiments. Two stop-flow spectrometers, one fixed wavelength, the other rapid scanning, were employed in the kinetics experiments. The fixed wavelength instrument (Atom-Mech Machine Co., Long Island, N.Y.), similar in design to that of Sutin,[28] was interfaced to a Raytheon 706 computer system for acquisition of intensity-time data.[27] Typically 300 data points were acquired per reaction decay.

The rapid scanning stop-flow kinetic spectrometer was a combination of a commercial rapid scan spectrometer (RSS) (Harrick Scientific Corp., design by Kuwana),[29] a locally designed stop-flow drive, and the same mixing cell as the fixed wavelength instrument. A Raytheon 706 computer system was used to control the RSS and to acquire the spectral data during reaction decay. The spectral acquisition rate could be as fast as a 50-point 250-nm spectrum taken in 1.20 ms with a repetition rate of 2 ms. Typically 100 50-point spectra were taken during decay. The recorded spectra can be plotted out and inspection made for intermediate (none found) and product absorptions and isosbestic points. Events at a given wavelength can be extracted from the spectral data set and examined as a function of time in the same manner as data obtained on the fixed wavelength instrument. A complete description of the computer-controlled stop-flow RSS has been published.[30] All kinetic data are averages of 3–6 runs.

Kinetic Data Analysis. The most useful spectral response for both quinones is the decay of the quinone radical anion absorption band. This band does not decay to zero, as the protonation reactions are reversible and usually do not proceed to completion. This reversibility was a factor in the data analysis, which was carried out using two approaches.

In the first, the forward rate differential equation is integrated and the integral arranged as a linear time function in the conventional manner.[31] The data are plotted according to these expressions, and the rate constants determined from the plot's slope over the first reaction half-life, hopefully before the buildup of products has induced a significant back reaction. The postulated reaction order is confirmed if the rate constant measured in this way shows the expected behavior over a range of initial reactant concentrations. The rate law plots show nonlinearity at longer times, due to the back reaction, and useful information is not obtained there.

The second method of data analysis involves a numerical integration of the postulated rate law, including the back reaction terms, by the Runge Kutta technique, which is well suited for solving complex kinetic expressions.[32,33] A large number of radical absorbance decays for DAQ were simulated by this approach for various rate laws and were compared with the experimental decays for a wide range of initial reactant concentrations. These comparisons served to confirm the reaction mechanism implied by the results of the first data analysis approach.

Cyclic Voltammetry. Cyclic voltametric experiments were conducted in a small volume (20 ml) cell with 0.0136 cm^2 hanging mercury drop working electrode, concentric Pt coil auxilary electrode, and Luggin aqueous SCE. Peak potentials were reproducible to 0.01 V. Supporting electrolyte was 0.5 M tetrabutylammonium perchlorate.

Table I. Spectral Data for AQ and DAQ in DMF with 0.1 M $TBA^+ClO_4^-$

	DAQ		AQ	
Species	λ_{max}, nm	$\epsilon \times 10^{-3}$ M^{-1} cm^{-1}	λ_{max}, nm	$\epsilon \times 10^{-3}$ M^{-1} cm^{-1}
Neutral quinone	431	10.1	326	5.8
Radical anion	302		297	
	373	5.0	392	5.2
	448	9.6	413	5.5
	542	7.7	556	11.2
Dianion	438	15.4	503	13.9
Hydroquinone anion	417	16.5		
Hydroquinone	401		384	7.4
	448		420	4.8

Results and Discussion

The quinones 1,8-dihydroxy-9,10-anthraquinone (DAQ) and 9,10-anthraquinone (AQ) in DMF with $TBA^+ClO_4^-$ supporting electrolyte each exhibit two reversible electrochemical reduction steps. For DAQ, the waves appear at −0.55 and −1.23 V; for AQ at −0.82 and −1.49 V vs. SCE, as in prior reports.[7,34,35] The two waves represent generation of radical anion and dianion, respectively,[36-38] confirmed by our OTTLE electrolysis showing $n = 1$ on both waves. From the potential separation of the two waves K_{disp} for reaction 6 is

$$2DAQ^{\cdot -} \rightleftarrows DAQ^{2-} + DAQ \qquad K_{disp} = 3.1 \times 10^{-12} \quad (9)$$

$$2AQ^{\cdot -} \rightleftarrows AQ^{2-} + AQ \qquad K_{disp} = 4.4 \times 10^{-12} \quad (10)$$

Addition of benzoic acid ($pK_a = 12.3$ in DMF)[39] increases the current on the first reduction wave of both quinones at the expense of the second wave, resulting, at sufficiently high acid concentration, in a single two-electron wave. The classical interpretation of this behavior is in terms of reactions 1–4.

With this electrochemical background we proceed to characterize the spectra and stoichiometry of $DAQ^{\cdot -}$ and $AQ^{\cdot -}$ in their respective reactions with benzoic acid (HBz).

Spectra and Stoichiometry for DAQ. Table I summarizes spectral results for DAQ and its various reduced and protonated forms. The data resemble those for 1-hydroxy-9,10-anthraquinone, as expected.[40] Spectra of $DAQ^{\cdot -}$ and DAQ^{2-} were obtained by OTTLE electrolysis at −0.8 and

−1.4 V. The spectra of $HDAQ^-$ obtained from OTTLE electrolysis at −0.8 V in the presence of HBz was identical for 1:1 through a 50:1 excess of HBz. This demonstrates that the reaction of $DAQ\cdot^-$ with HBz stops at the monoprotonated stage:

$$2DAQ\cdot^- + HBz \rightleftarrows HDAQ^- + DAQ + Bz^- \quad (11)$$

Confirmation is obtained by comparing batch spectra of $DAQ\cdot^-$ mixed with 0.5:1 and 24:1 $HClO_4$ and HBz, respectively. Except for residual $DAQ\cdot^-$ absorbance at 448 and 542 nm (vide infra), these spectra are identical. In the $HClO_4$ experiment, protonation is stoichiometrically limited to $HDAQ^-$. The $HDAQ^-$ spectrum produced in the 0.5:1 $HClO_4$ batch experiment is furthermore accurately reproduced by a 1/1 summation of $HDAQ^-$ and DAQ OTTLE spectra.[27]

With a 7.5:1 excess of $HClO_4$, a new species, which we believe to be diprotic H_2DAQ, appears. Since the spectrum of 1:1 $DAQ\cdot^-/HClO_4$ retains a substantial contribution from $HDAQ^-$, H_2DAQ must be an exceptionally strong acid in DMF. The low proton affinity of $HDAQ^-$ can be interpreted as a reflection of bonding of the 9-oxygen with the two hydroxyl functions.[38]

The radical anion spectrum is insensitive to water concentration, on an OTTLE time scale, up to 0.1 M added water in DMF.

Spectra and Stoichiometry of AQ. Spectral data for AQ and its various reduced and protonated forms (Table I) agree with previous results.[35] Spectra of $AQ\cdot^-$ and AQ^{2-} were obtained by OTTLE electrolysis, as was that of H_2AQ by two-electron reduction at −1.0 V in the presence of stoichiometric (2:1) or greater concentrations of $HClO_4$ and HBz. The H_2AQ spectrum was identical for both acids. Batch spectral experiments in which $AQ\cdot^-$ was mixed with 2:1 or greater HBz gave a spectrum which was a 1:1 composite of the AQ and H_2AQ OTTLE spectra.

With less than 2:1 amounts of HBz, OTTLE electrolysis spectra showed only $AQ\cdot^-$ and H_2AQ. In a series of experiments with differing [HBz], the concentration of $AQ\cdot^-$ as monitored at 556 nm decreased linearly with increasing HBz concentration, titrating to zero radical anion at a 2:1 ratio. Also, the coulometric charge for reduction of a 1:1 mixture of HBz and AQ was determined by OTTLE. If the product is HAQ^-,

$$AQ + HBz + 2e \rightarrow HAQ^- + Bz^- \quad (12)$$

then $n = 2.0$. If on the other hand only H_2AQ and $AQ\cdot^-$ are produced,

$$AQ + HBz + 1.5e \rightarrow \tfrac{1}{2}H_2AQ + \tfrac{1}{2}AQ\cdot^- + Bz^- \quad (13)$$

the expected $n = 1.5$. The latter result was obtained. The data are all consistent with $AQ\cdot^-$ protonation by HBz proceeding exclusively to the diprotonated H_2AQ stage. Evidently, $AQ\cdot^-$ is a weaker base than HAQ^-, but the latter is a stronger base relative to Bz^-.

Equilibrium of $DAQ\cdot^-$ Protonation Reaction. When DAQ is electrolyzed in the presence of excess HBz, the protonation reaction is driven to completion by continued reduction of DAQ. In the absence of the electrochemical driving force, as in stop-flow mixing of $DAQ\cdot^-$ solutions with HBz, the protonation reaction 11 does not proceed to completion even in excess HBz. Residual $DAQ\cdot^-$ is clearly apparent in the product solutions (by a band at 542 nm). The extent and rate of consumption of $DAQ\cdot^-$ are both retarded by adding products DAQ or Bz^-. Thus reaction 11 is reversible with a modest equilibrium constant (K_{HDAQ^-}).

$$K_{HDAQ^-} = [DAQ][Bz^-][HDAQ^-]/[DAQ\cdot^-]^2[HBz] \quad (14)$$

Table II. Equilibrium Constant K_{HDAQ^-} for DAQ Radical Anion Protonation

Initial concentrations					
$[DAQ\cdot^-]$, mM	[HB], mM	[DAQ], mM	$[Bz^-]$, mM	$K_{HDAQ^-} \times 10^2$	α^a/β
0.20	2.4	0.0	0.0	1.23	1.30
		1.8		2.31	0.94
		3.2		2.90	1.07
0.20	9.6	0.0	0.0	1.85	0.99
		0.20		1.77	0.92
		0.80		1.76	0.94
		1.8		2.48	1.13
		3.2		2.29	1.12
		0.0	0.20	2.43	0.90
			0.80	2.45	0.89
			1.6	2.09	0.92
			3.2	1.44	0.97
		0.20	0.20	1.95	0.94
		0.40	0.40	2.07	1.20
0.30	3.6	0.0	0.0	1.60	0.94
		1.2		1.89	0.99
		4.8		1.72	
0.30	14.4	0.0	0.0	1.72	0.93
		0.30		2.21	1.06
		1.2		2.56	1.32
		2.7		1.64	1.27
		4.8		2.40	1.47
Mean value 2.01×10^{-2} (std dev 0.42) Rel std dev 21%					

[a] See text following eq 21 for explanation.

Evaluation of K_{HDAQ^-} is necessary for the kinetic study of reaction 11. An accurate assessment requires inclusion of the benzoate-benzoic acid homoconjugation equilibrium:

$$HBz + Bz^- \rightleftarrows HBz_2^- \quad (15)$$

$$K_{HBz_2^-} = [HBz_2^-]/[HBz][Bz^-]$$

Knowing the reaction stoichiometry, evaluating $[DAQ\cdot^-]_{t=0}$, and following reaction of known amounts of $DAQ\cdot^-$ with HBz in the presence of various added amounts of DAQ and Bz^- are sufficient to ascertain all terms in the K_{HDAQ^-} expression. The value of $K_{HBz_2^-}$ at $\mu = 0$ is 250 M^{-1}.[39] While K_{HDAQ^-} is not highly sensitive to $K_{HBz_2^-}$, a value of 200 M^{-1} gave a better fit to the combined equilibrium equations 14 and 15. Table II gives results for K_{HDAQ^-} over a wide range of initial concentrations and products. The small value of 0.020 for K_{HDAQ^-} shows that $DAQ\cdot^-$ is, in fact, a rather weak base.

Evaluation of K_{HDAQ^-}, together with the known pK_{HBz} for benzoic acid[39] and K_{disp} for DAQ (vide supra), incidentally allows calculation of the acid dissociation constant $K_{a,2}$ for $HDAQ^-$ in DMF solvent

$$K_{a,2} = \frac{[H^+][DAQ^{2-}]}{[HDAQ^-]} = \frac{K_{HBz}K_{disp}}{K_{HDAQ^-}} = 8.4 \times 10^{-23} \quad (16)$$

By comparison, phenol ($pK_a = 18$)[41] is a much stronger acid, and consequently OTTLE spectra of $HDAQ^-$ can be observed by electrolysis of DAQ on its second wave in the presence of phenol.

Equilibrium of $AQ\cdot^-$ Protonation Reaction. When $AQ\cdot^-$ is flow mixed with HBz, small amounts of $AQ\cdot^-$ are apparent in the product spectrum, but not as much as in the $DAQ\cdot^-$ case. Greater amounts of residual $AQ\cdot^-$ are apparent if it is mixed with HBz with added Bz^- or AQ. To determine the effect of this obvious back reaction on the kinetic data, it was necessary to ascertain the value of the

Table III. Equilibrium Constant K_{H_2AQ} for AQ Radical Anion Protonation

Initial Concn			Equilibrium concn	
[AQ·⁻], mM	[HB], mM	[AQ], mM	[AQ·⁻], mM	$K_{H_2AQ} \times 10^{-2}$
0.10	0.15	0.0	0.004	4.09
		0.20	0.007	6.20
		0.45	0.016	1.29
		0.80	0.021	0.96
0.20	0.30	0.00	0.011	2.07
		0.20	0.016	2.76
		0.80	0.018	6.30
		1.6	0.024	5.18
0.30	0.45	0.0	0.013	3.92
		1.2	0.047	1.28
		2.4	0.051	1.89

Mean value 3.3×10^2
Std dev 2.0
Rel std dev 61%

equilibrium constant for the reaction:

$$2AQ\cdot^- + 2HBz \rightleftarrows H_2AQ + AQ + 2Bz^- \qquad (17)$$

$$K_{H_2AQ} = [H_2AQ][AQ][Bz^-]^2/[AQ\cdot^-]^2[HBz]^2$$

As with DAQ, the value of $K_{HBz_2^-} = 200\ M^{-1}$ (eq 16) was used in the data fit. The protonation equilibrium constant is much larger for AQ, and determination of small residual AQ·⁻ concentrations (4–16%) causes greater uncertainty in the evaluated constant, which is 330 ± 200. The data are displayed in Table III.

The overall acid dissociation constant, $K_{a,1}K_{a,2}$ for H_2AQ can be, incidentally, calculated from the K_{H_2AQ} result:

$$K_{a,1}K_{a,2} = \frac{[H^+]^2[AQ^{2-}]}{[H_2AQ]} = \frac{K_{HBz}^2 K_{disp}}{K_{H_2AQ}} = 4.1 \times 10^{-39} \qquad (18)$$

Since the protonation data imply that for AQ, $K_{a,1} < K_{a,2}$, it follows that $K_{a,2} > 6 \times 10^{-20}$. When compared with $K_{a,2}$ for $HDAQ^-$, this implies that HAQ^- is a much stronger acid than $HDAQ^-$.

Kinetics and Mechanism for DAQ·⁻ Protonation by HBz. In reaction sequences 2,5 and 6,7, the protonation of DAQ·⁻ proceeds via an intermediate species (HDAQ· and DAQ^{2-}, respectively). We have made extensive use of the RSS–stop flow in an attempt to detect transient bands, in the DAQ·⁻ protonation reaction, with negative results. The expected isosbestic point at 433 nm is observed throughout the reaction and is invariant with initial reactant concentration. Further, DAQ·⁻ disappears (542 nm) and $HDAQ^-$ appears (417 nm) at identical rates. The lifetime and population of any intermediate in the protonation reaction is very small. We accordingly employ a steady-state approximation for intermediates in the mathematical analysis of various reaction sequences.

To determine the order of reaction in radical anion, anion radical absorbance decays were examined by standard plots of integrated rate equations for simple first- and second-order behavior. The examination was conducted for three different radical anion concentrations and at HBz concentrations sufficiently high that changes in [HBz] during the reaction could be neglected. Both first- and second-order rate plots curve toward slower rates at longer times, a consequence of the back reaction. For HBz excesses so large (50×) that the protonation reaction is driven to near completion, however, second-order plots approach linearity (Figure 1). Further, the rate constant extracted over the

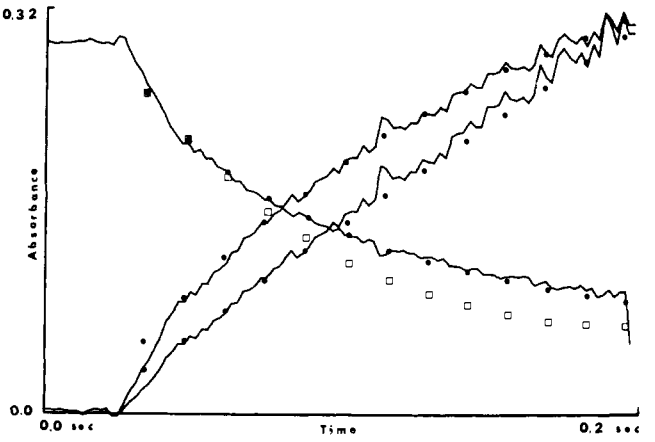

Figure 1. Reaction of 0.2 mM DAQ·⁻ with 9.6 mM HBz measured at 542 nm. Descending trace: observed reaction decay; ascending traces: upper, analysis for first-order decay of radical anion, abscissa is ln $\{[DAQ\cdot^-]_0/[DAQ\cdot^-]_t\}$; lower, analysis for second-order decay of radical anion, abscissa is $(1/[DAQ\cdot^-]_t - 1/[DAQ\cdot^-]_0)$. ● indicate, for proposed reaction mechanism 19, 20, simulated reaction decay and analysis of that decay. □ indicate simulated reaction for a reversible reaction whose forward rate is first order in both DAQ·⁻ and HBz.

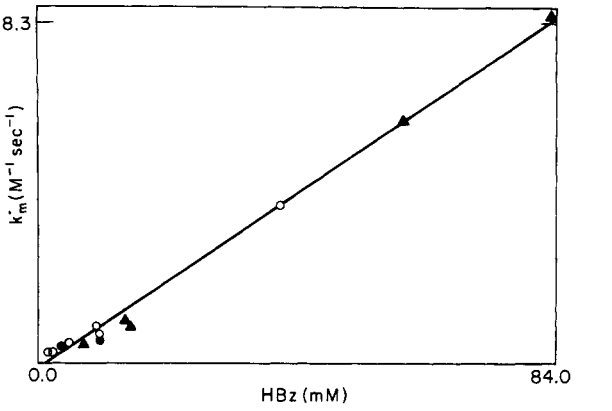

Figure 2. Linear dependence of rate constants $k_m' \times 10^4\ M^{-1}\ s^{-1}$ (obtained by analysis assuming second-order behavior in DAQ·⁻) on acid concentration (least-squares line): [DAQ·⁻] = 0.2 mM, ○; 0.3 mM, ▲; 0.4 mM, ●.

first half-life of second-order plots is constant with different initial radical anion concentrations. These results, supplemented by evidence presented later, lead us to conclude that the reaction is second order in DAQ·⁻.

To evaluate the reaction order in acid, rate constants k_m' obtained from the first half-life of plots second order in radical are plotted against [HBz] in Figure 2, whose linearity demonstrates that the reaction is first order in benzoic acid. Next, all radical anion absorbance decays were plotted for an integrated rate equation first order in acid and second order in radical anion (which is applicable to reactions where HBz is not necessarily present in large excess). Rate constants, k_{meas}, obtained over the first one and two half-lives of this plot are given in Table IV. The values taken over the first reaction half-life show a satisfactory degree of constancy over the range of concentrations employed. This evaluation is, of course, for the forward rate only.

Third-order behavior in the reactants implies, mechanistically, an unfavorable equilibrium, followed by a rate-controlling step. This would in the known reaction sequences 2,5 and 6,7 mean that the second step of each exerts rate control. Experimental data were unsuccessfully compared with the corresponding rate law of each sequence. For sequence 2,5, the forward-reaction rate-law term contains an

Table IV. Rate Constants Obtained for DAQ·⁻ Protonation from a Rate Plot Second Order in Radical Anion, First Order in Acid

[DAQ·⁻] mM	[HBz], mM	k_{meas} for first half-life × 10^{-6} M^{-2} s^{-1}	k_{meas} over 2 half-lives × 10^{-6} M^{-2} s^{-1}
0.20	0.40	12.2	5.46
	0.80	9.54	5.46
	1.6	9.03	6.84
	5.0	7.96	5.55
	9.6[a]	8.25	6.78
	10.0	5.90	5.93
	40.0	6.32	9.28
0.30	1.2	9.52	4.85
	2.4	6.67	4.81
	3.6[a]	8.25	6.15
	7.5	4.88	4.85
	14.4[a]	6.51	5.20
	15.0	5.08	5.32
	21.0	4.36	4.66
	30.0	4.12	4.45
	60.0	8.40	9.67
	84.6	11.6	9.86
0.40	0.80	5.10	4.39
	1.6	6.42	3.81
	3.2	5.48	8.09
	10.0	4.63	3.19
	Weighted mean 7.3×10^6 M^{-2} s^{-1}		
	Std dev 2.2×10^6 M^{-2} s^{-1}		

[a] Reaction studied with RSS-SF.

inverse dependence on [Bz⁻], in addition to second-order dependence on radical anion and first order on HBz. Experimental data analyzed over the first half-life by a plot of the integrated form of this term gave rate constants which decreased with increasing [HBz] by over two powers of ten. Also, in experiments with excess [Bz⁻], added with the acid reactant solution, effects of the back reaction are more prominent, but the forward rate constant does not depend inversely on [Bz⁻]. In reaction sequence 6,7 for DAQ·⁻, the forward reaction term of the rate law contains an inverse dependence on [DAQ]. An analysis for such dependence follows lines like that for the inverse [Bz⁻] dependency above, again with negative results. Furthermore, the rate constant typically obtained, 10^{14} M^{-1} s^{-1}, exceeds the limits of diffusion control.

Sequences 2,5 and 6,7, mechanisms accepted as alternative to ECE behavior, do not satisfy the data for DAQ·⁻ protonation. Sequence 2,5 retains its chemical appeal, however. We propose a new protonation sequence in which the flawed [Bz⁻] dependence of sequence 2,5 is circumvented by assuming that the protonation step is not accompanied by benzoate loss, but that the radical anion and benzoic acid form a transient heteroconjugate acid–base dimer which is subsequently reduced by radical anion in the rate-limiting step. Radical anion–acid complexes have previously been observed in aprotic solvents in ESR measurements.[42-45]

The proposed reaction mechanism is

$$DAQ\cdot^- + HBz \underset{k_{-4}}{\overset{k_4}{\rightleftharpoons}} \{DAQ \cdots HBz\}\cdot^- \qquad K_4 = k_4/k_{-4} \tag{19}$$

$$\{DAQ \cdots HBz\}\cdot^- + DAQ\cdot^- \underset{k_{-5}}{\overset{k_5}{\rightleftharpoons}} HDAQ^{\cdot-} + DAQ + Bz^- \qquad K_5 = k_5/k_{-5} \tag{20}$$

Assuming a steady-state approximation for the acid–radical anion complex, the following rate law is obtained:

$$\frac{-d[DAQ\cdot^-]}{dt} = 2K_4k_5[DAQ\cdot^-]^2[HBz^-] - 2k_{-5}[HDAQ^-][DAQ][Bz^-] \tag{21}$$

The forward rate term of eq 21 is second order in radical anion and first order in acid, which corresponds to the result of Table IV. In order to evaluate this rate law more fully, an analysis of the effect of the back reaction was carried out by Runge Kutta numerical calculations of eq 21 to simulate experimental decays of [DAQ·⁻] for a large variety of reactant and product initial concentrations. The value of 7.3×10^6 M^{-2} s^{-1} from Table IV was employed for $2K_4k_5$, that for k_{-5} was calculated from $2K_4k_5$ and $K_{HDAQ^-} = K_4K_5 = 0.020$, and instantaneous [HBz] and [Bz⁻] were corrected for homoconjugate formation by eq 15. The simulated radical anion decays match the actual experimental decays very well both when only DAQ·⁻ and HBz are present initially, the back-reaction then arising from gradual product build-up (Figures 1 and 3), and when DAQ and/or Bz⁻ were added to the initial reactants to accentuate the back reaction (Figure 3). (The figures shown are roughly 10% of the total collection of comparisons made.) Further, when decay data simulated from eq 21 for a reaction where no DAQ or Bz⁻ products were initially present are plotted according to a simple second-order decay in radical anion, exactly the same curvature arises in this "analysis" of theoretical data as arises in the same analysis of the corresponding experimental data. An example is shown in Figure 1. This demonstrates that the curvature of the radical anion second-order analysis plots is accounted for quantitatively by a back reaction effect.

Lastly, in order to provide a numerical basis for the "goodness of fit" of the simulated to experimental data, plots of both data sets were made according to the integrated form of the forward rate term of eq 21 (second order in radical, first order in acid). The average slope of these plots (curved at longer times because of the neglect of the back reaction term) was computed over an arbitrary time period (200 ms). A slope ratio $\alpha/\beta = 1.0$ implies a good match; most of the comparisons fall within 10% of this value (Table II).

All of these results are consistent with the proposed reaction sequence 19,20, which is the only mechanism we have conceived which is fully consistent with experimental facts. Several other attempts at analysis of the kinetic data should be mentioned in this connection. Our initial anticipation in this study was sequence 2,5 with rate control by reaction 2, which would make the reaction first order in anion radicals. While the integrated rate equation plots indicated that this was not so, we nonetheless prepared a series of Runge Kutta simulations of experimental data based on a reversible reaction sequence 2,5 and first order in radical. We found that a single rate constant was inadequate over a range of reaction and product concentration to produce a uniformly good match between simulated and experimental decays. When the forward rate was adjusted for a best fit over the first half-life, the reverse rate required by this value and K_{HDAQ^-} led to a simulated decay which always diverged from the experimental at longer times. An example of this discordancy is shown by the open squares in Figure 1. Other reaction steps considered and also discarded were (i) predissociation of HBz (pK_{HBz} is so small that the value of k_{meas} requires the electron-transfer reaction 5 to exceed the diffusional limit) and (ii) disproportionation of HDAQ· or [DAQ···HBz]·⁻ (overall reaction would have to be second order in HBz).

Kinetics and Mechanism for AQ·⁻ Protonation by HBz. Spectral decays during protonation of anthraquinone anion

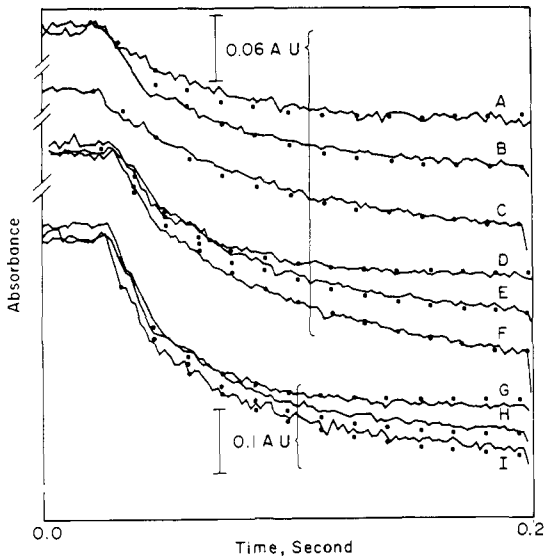

Figure 3. Experimental reaction decays (542 nm, solid lines) for protonation of DAQ·$^-$ by HBz compared with reaction decays simulated to proposed mechanism reactions 19, 20. curves A–F: DAQ·$^-$ = 0.2 mM, HBz = 9.6 mM; curve A, Bz^- = 0.2 mM, DAQ = 0.2 mM; curve B, Bz^- = 0.4 mM, DAQ = 0.4 mM; curve C, DAQ = 0.8 mM; curve D, Bz^- = 3.2 mM; curve E, Bz^- = 0.8 mM; curve F, no added products. curves G–I: DAQ·$^-$ = 0.3 mM, HBz = 14.4 mM; curve G, DAQ = 4.8 mM; curve H, DAQ = 0.3 mM; curve I, no added products.

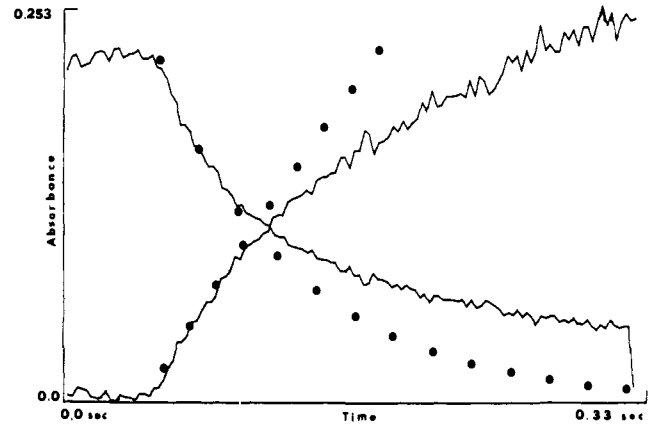

Figure 4. Reaction of 0.1 mM AQ·$^-$ with 0.5 mM HBz measured at 556 nm. Descending trace: observed reaction decay; ascending trace: kinetic analysis first order in AQ·$^-$ and in HBz, abscissa is $\{1/([HBz]_0 - [AQ\cdot^-]_0)\} \ln \{[AQ\cdot^-]_0[HBz]_t/[AQ\cdot^-]_t[HBz]_0\}$. ● are for simulated reaction (first order in AQ·$^-$ and HBz, reversible, affected by homoconjugation) and the corresponding analysis for its behavior.

radical (AQ·$^-$) by benzoic acid (HBz) were carefully examined but lacked any evidence of transient intermediates. Two isosbestic points at 426 and 456 nm are invariant with time and reactant concentrations, and rates of disappearance of AQ·$^-$ at four wavelengths (392, 413, 510, 556 nm) and of appearance of H_2AQ at 430 nm are all the same. This information allows us to use a steady-state approximation for any intermediates.

The equilibrium constant for AQ·$^-$ protonation (Table III) is substantially larger than for DAQ·$^-$. Back reaction effects still had to be dealt with, however, as the more reliable protonation data were obtained at [HBz] not $\gg$[AQ·$^-$]. At high [HBz], the AQ·$^-$ protonation reaction velocity was so large that the reaction is nearly over before the solution becomes transported from mixing to observation point in the stop-flow instrument (see third column, Table V).

Analysis of AQ·$^-$ decays in which at least 70% of the reaction is observable by an integrated rate expression for first order AQ·$^-$/first order HBz decay gives rate constants over the first half-life that are constant over a range of [AQ·$^-$] and [HBz] (see Table V). At longer times, the rate plots curve down (slower rate), an expected qualitative consequence of the reaction's reversibility. Quantitatively, however, this curvature exceeds that accountable by back reaction, as the simulation–experiment comparison of Figure 4 illustrates. In short, we find the reaction to be first order in both AQ·$^-$ and HBz early in the reaction, but the reaction order appears to increase later in the reaction.

The AQ·$^-$ protonation decays were also scrutinized using integrated rate expressions which were (i) second order in AQ·$^-$/first order in HBz, and (ii) second order in AQ·$^-$/first order in HBz/inverse first order in Bz^-. The former of these had proved satisfactory for DAQ·$^-$ protonation. Neither analysis was satisfactory for AQ·$^-$, both gave rate plots curving *up* with time (unexplainable by a back reaction effect). The former also gave first half-life rate constants decreasing at higher initial [AQ·$^-$].

The addition of excess benzoate to the AQ·$^-$ protonation reaction greatly diminishes the reaction velocity. In the presence of excess Bz^-, we furthermore now find that integrated rate equation plots second order in AQ·$^-$/first order in HBz/inverse first order in Bz^- are fairly linear and are independent of the initial [HQ·$^-$], [HBz], or [Bz^-]. Results are given in Table VI. Homoconjugation (HBz_2^-) was accounted for in the rate plots. The slight downward curvature in the rate plots is due to the back reaction effect. An experimental example is shown in Figure 5. In both Table VI and Figure 5, [Bz^-] is sufficiently high as to be considered constant. Addition of excess parent AQ to the reaction, in contrast, has only the slight rate-retarding effect expected for enhancement of the overall back reaction.

We interpret the above as follows. Reaction sequence 2,5,4, written for AQ·$^-$ is

Table V. Rate Constants Obtained for AQ·$^-$ Protonation from a Rate Plot First Order in Both AQ·$^-$ and HBz

[AQ·$^-$] mM	[HBz] mM	$[AQ\cdot^-]_{t=0}$[a] mM	k_{meas} for first half-life × 10^{-4} M^{-1} s^{-1}
0.055	0.33	0.041	2.58[c]
0.083	0.054	0.068	3.02[c]
0.10	0.15	0.092[b]	2.38[c]
	0.25	0.091[b]	2.95[c]
	0.5	0.078[b]	2.75[c]
	1.5	0.067[b]	2.62
	2.5	0.056	1.22
	5.0	0.021	0.91
0.11	0.33	0.10	2.95[c]
	0.66	0.082	2.16[c]
0.20	0.2	0.19	3.36[c]
	0.3	0.18[b]	3.73[c]
	0.4	0.18	1.70[c]
	0.5	0.16[b]	4.29[c]
	1.0	0.16[b]	2.88[c]
	1.6	0.12	1.45
0.30	0.45	0.26[b]	4.86[c]
	0.75	0.24[b]	3.86[c]
	1.5	0.21[b]	3.72
	2.4	0.10	1.69
	4.8	0.062	1.12

[a] $[AQ\cdot^-]_{t=0}$ is the amount of radical anion observed initially. [b] Measured with RSS-SF. [c] At least 70% of reaction decay observed; weighted mean of these rates is $3.10 \pm 0.65 \times 10^4$.

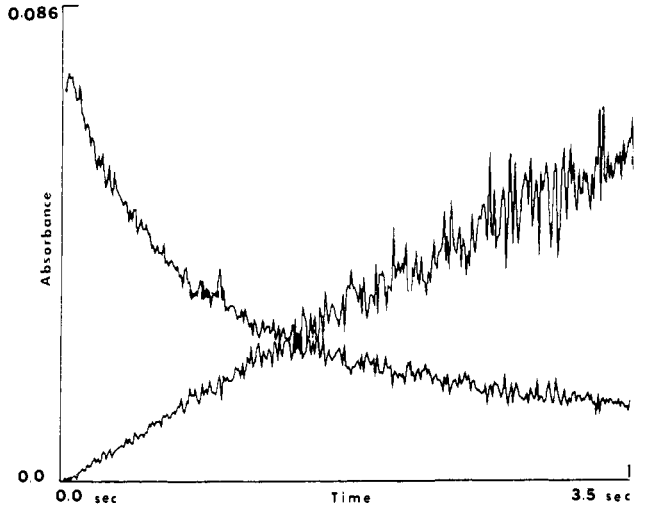

Figure 5. Reaction of 0.055 mM $AQ\cdot^-$ with 0.33 mM HBz and 1.1 mM Bz^- measured at 556 nm. Descending trace: observed reaction decay; ascending trace: kinetic analysis second order in $AQ\cdot^-$, first order in HBz, and inverse first order in Bz^-, abscissa is

$$\left\{\frac{1}{[HBz]_0 - [AQ\cdot^-]_0}\right\}\left\{\frac{1}{[AQ\cdot^-]_t} - \frac{1}{[AQ\cdot^-]_0}\right\} + \left\{\frac{1}{[HBz]_0 - [AQ\cdot^-]_0}\right\}^2 \ln\left\{\frac{[HBz]_0[AQ\cdot^-]_t}{[HBz]_t[AQ\cdot^-]_0}\right\}$$

Table VI. Rate Constants for $AQ\cdot^-$ Protonation in the Presence of Added Benzoate from a Rate Plot Second Order in Radical Anion, First Order in Acid, and Inverse Order in Benzoate[a]

Initial concn			Equilibrium concn	$k_{meas} \times 10^{-5}$ M^{-1} s^{-1}	
$[AQ\cdot^-]$, mM	[HBz], mM	$[Bz^-]$, mM	$[AQ\cdot^-]_{Eq}$, mM	First half-life	Overall
0.055	0.33	1.1	0.006	1.4	1.3
		2.2	0.013	1.6	1.5
0.083	0.54	1.67	0.010	1.7	1.5
		3.3	0.021	1.9	1.4
0.11	0.33	1.1	0.016	1.1	0.9
		2.2	0.029	1.3	1.0
	0.66	2.2	0.14	1.6	1.2
		4.4	0.029	2.0	1.2

[a] Rates are corrected for homoconjugate formation with a value of 200 M^{-1} s^{-1} for $K_{HBz_2^-}$

$$AQ\cdot^- + HBz \underset{k_{-6}}{\overset{k_6}{\rightleftharpoons}} HAQ\cdot + Bz^- \qquad K_6 = k_6/k_{-6} \qquad (22)$$

$$HAQ\cdot + AQ\cdot^- \underset{k_{-7}}{\overset{k_7}{\rightleftharpoons}} HAQ^- + AQ \qquad K_7 = k_7/k_{-7} \qquad (23)$$

$$HAQ^- + HBz \rightleftharpoons H_2AQ + Bz^- \qquad K_8 \qquad (24)$$

Since HAQ^- is not observed, K_8 can be considered a labile and favorable equilibrium. Assuming that $K_{H_2AQ} = K_6K_7K_8$ and a steady-state approximation for [HAQ·], the general rate law is

$$\frac{-d[AQ\cdot^-]}{dt} = \frac{2k_6\{[AQ\cdot^-]^2[HBz] - ([H_2AQ][AQ][Bz^-]^2/[HBz]K_{H_2AQ})\}}{(k_{-6}/k_7)[Bz^-] + [AQ\cdot^-]} \qquad (25)$$

When $(k_{-6}/k_7)[Bz^-] > [AQ\cdot^-]$ (as when excess Bz^- is added), the forward rate is second order in $AQ\cdot^-$, first order in HBz, and inverse first order in Bz^-, which is in accord with experiment. For this model, the first half-life k_{meas} of Table VI (1.6×10^5 M^{-1} s^{-1}) is $2K_6k_7$. When no Bz^- is added and its initial concentration is low, eq 25 shows that the forward rate can then initially be first order in $AQ\cdot^-$ and HBz, but subsequently change, as Bz^- builds up, according to the magnitude of k_{-6}/k_7. The forward reaction rate constant early in the reaction in the low $[Bz^-]$ case is $2k_6$, which is $k_{meas} = 3.10 \times 10^4$ M^{-1} s^{-1} of Table V. We have previously noted that the rate plots from which k_{meas} of Table V are derived curve down toward a higher order decay of $AQ\cdot^-$, which is consistent with eq 25.

Table VII. Rate Constants for $AQ\cdot^-$ Protonation in Absence of Added Bz^- from a Plot of Eq 26 Using 5.2 for k_7/k_{-6}

Initial concn		$2K_6k_7 \times 10^{-5}$ M^{-1} s^{-1}	
$[AQ\cdot^-]$, mM	[HBz] mM	First half-life	Overall
0.055	0.33	1.4	1.5
0.83	0.54	1.5	1.6
0.1	0.15[a]	1.1	0.9
	0.25[a]	1.4	1.2
	0.5[a]	1.3	0.8
	2.5	0.8	0.8
0.11	0.66	1.1	1.3
0.2	1.0[a]	1.5	1.2
	1.6	0.9	1.0
0.3	0.45[a]	2.2	1.3
	0.75[a]	1.9	1.1
	1.5[a]	1.5	0.8
	2.4	1.3	1.1
	4.8	1.3	1.2

[a] Measurement on RSS-SF.

Integration of the forward reaction component of eq 25 and rearranging gives

$$2K_6k_7t = \frac{1}{([HBz]_m - [AQ\cdot^-]_m)\psi}\left\{\frac{[AQ\cdot^-]_m - [AQ\cdot^-]}{[AQ\cdot^-]} + \left[\frac{[HBz]_m}{[HBz]_m - [AQ\cdot^-]_m} - \frac{\psi k_7}{k_{-6}}\right] \times \ln\left[\frac{[HBz]_m\,[AQ\cdot^-]}{[AQ\cdot^-]_m[HBz]}\right]\right\} \qquad (26)$$

in which the subscript m denotes an initial reactant concentration, $[Bz^-]_m = 0$, and $\psi = 1 + [HBz]_mK_{HBz_2^-}$. There are two unknown terms in this equation, $2K_6k_7$ and k_7/k_{-6}. The k_7/k_{-6} term can be estimated as 5.2 from the ratio of k_{meas} of Tables V and VI. Using this value for k_7/k_{-6}, analysis of several sets of kinetic data obtained without added benzoate was carried out for eq 26 with results shown in Table VII. The fit is quite good, and the average value of $2K_6k_7$ (1.4×10^5 M^{-1} s^{-1}) is in good agreement with the value found (Table VI) for $2K_6k_7$ with excess benzoate (1.6×10^5 M^{-1} s^{-1}). The slight decrease in rate constant with time is expected since eq 26 leaves out the back reaction term.

These results show that the protonation mechanism for $AQ\cdot^-$ is adequately given by sequence 22,23,24, provided that we recognize that overall rate control can pass from reaction 22 to reaction 23 depending on $[Bz^-]$. This causes the order of reactants to change during the course of reaction.

Discussion and Comparison of $DAQ\cdot^-$ and $AQ\cdot^-$ Protonation Mechanisms. We have seen that protonation of $DAQ\cdot^-$ by HBz involves a fast but unfavorable equilibrium forming a heteroconjugate acid-base dimer whose consumption by reduction by fresh $DAQ\cdot^-$ constitutes overall reaction ve-

locity control (reactions 19,20). In the case of $AQ\cdot^-$, a dimer is not formed. The proton is instead transferred completely in a rate-controlling step in the absence of its anionic product, with overall reaction velocity control shifting to reduction of HAQ· by fresh $AQ\cdot^-$ as Bz^- accumulates, or is added (reactions 22-24).

Both of these mechanistic situations differ in detail from those uncovered in previous stop-flow observations of radical anion protonations[15-20] They are likewise very different from the mechanistic statements implicit in the usual electrochemical ECE sequence (reactions 1-4 or 1, 2, 5, 4), being reversible, exhibiting reaction control by the electron transfer rather than the proton-transfer step, exhibiting second-order radical decay, and exhibiting no significant population of neutral, protonated radical ($DAQ\cdot^-\cdots HBz$ or HAQ·). The latter means, electrochemically, that the concept of a radical anion diffusing from an electrode to be protonated to give a neutral radical with chemical lifetime long enough to return to the electrode may often be false.

It is perhaps, but not entirely, surprising that the two superficially similar quinones AQ and DAQ should exhibit different mechanistic characteristics. Both quinones are similar in that their protonation reactions exhibit low driving forces (both have a small reaction K_{eq}). Neither anion radical is a strong base with respect to benzoic acid. $DAQ\cdot^-$ has, in fact, basicity comparable with that of benzoate, leading to a heteroconjugate dimer formation. The $AQ\cdot^-$ basicity seems to be larger, and its heteroconjugate is not stable. This basicity difference undoubtedly derives from the intramolecular hydrogen bonding in $DAQ\cdot^-$.[38] In both cases the driving force for the overall reaction originates in the electron-transfer step, but the basicity difference forms the source of differences in reaction order and rate-controlling step. The $DAQ\cdot^-\cdots HBz$ dimer is formed rapidly without bond breaking, but in very small populations, which limits the electron-transfer step. With $AQ\cdot^-$, larger but nonobservable quantities of HAQ· are initially formed through the strong base action of $AQ\cdot^-$, and control rests with this step. If the population of HAQ· is diminished by Bz^- buildup or addition, then a low HAQ· population results which limits the electron-transfer rate.

It is, finally, pertinent to compare certain aspects of these results with previous radical anion protonation studies, summarized by Dye[20] for anthracenide in the presence of alkali metals in THF and DME. There, the more localized the radical's electron density (influenced by ion pairing), the faster the protonation rate. If electron density is highly localized, as in a tight ion pair, the energy for disproportionation of two radical anions is lowered, and protonation occurs through a dianion pathway (sequence 6,7). The effect of electron localization in tight ion pairs is illustrated by the difference in K_{disp} for $AQ\cdot^-$ in DMF/TBAP solution (4.4×10^{-12}, $AQ\cdot^-$ essentially a free ion),[46] and that of $K^+An\cdot^-$ in THF (1×10^{-5}, where tight ion pairs are favored).[20] Under conditions where loose ion pairs are formed (smaller value of K_{disp}), the rate-determining step becomes protonation of the radical anion and acid.[15,18-20,22] Reversibility of the overall reaction has not been encountered with either tight or loose ion pairs, and Dye[20] specifically found that the conjugate base of the protonating species has no effect on the reaction rate with $K^+An\cdot^-$. Our results are quite different with respect to the importance of the conjugate base. An examination of the fate of the conjugate base of the protonating acid can explain this particular difference. In systems with alkali metals, which are stronger Lewis acids than tetrabutylammonium ion, the conjugate base can become coordinated by the alkali cation, eliminating back reaction effects. This process of base removal is not available in our system and thus large effects on reaction rate

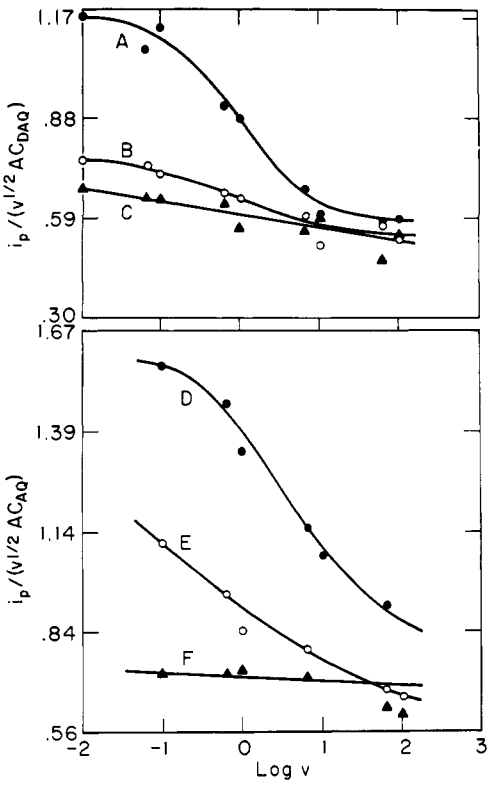

Figure 6. Upper: cyclic voltammetry current function vs. sweep rate for first wave in reduction of 0.5 mM DAQ in DMF; (A) with 2.5 mM HBz, (B) with 0.12 mM HBz, (C) no acid. Lower: cyclic voltammetry current function vs. sweep rate for first wave in reduction of 0.52 mM AQ in DMF; (D) with 2.5 mM HBz, (E) with 0.5 mM HBz, (F) no acid.

and equilibrium conditions as a result of benzoate are observed.

Electrochemical Characterization. Ideally, having the quinone radical anion protonation mechanism and rate in hand, one obtains quantitative electrochemical data under similar solution conditions to compare with electrochemical theory written for said mechanism. This gives a check for heterogeneous or other effects which might alter the mechanism in the electrochemical context. We chose not to take this step for these quinones, due to the complexity of the protonation mechanisms found. For $DAQ\cdot^-$, for instance, the reaction's reversibility plus second order in the radical represent new situations for electrochemical theory. We also uncovered some adsorption effects for these quinones at stationary electrodes in DMF which made highly precise mass transfer experiments difficult. Accordingly, we limit the electrochemical characterization to experiments designed to produce an approximate reaction half-life for comparison with stop-flow results.

Cyclic voltammetry of DAQ and AQ at mercury in the absence of acid shows a pair of one electron, chemically reversible waves for both quinones. The first wave is also electrochemically reversible (ΔE_{peak} = 62 and 65 mV, respectively). For both quinones these two waves are preceded by several small adsorption prewaves (i_{peak} proportional to sweep rate). The first diffusional wave increases less rapidly than expected with increasing sweep rate, indicating a relationship of quinone reactant to the adsorption waves. The first (radical-anion producing) wave was examined (Figure 6 C,F) as a function of sweep rate; a slight decrease for DAQ is due to the adsorption interference; the effect is less noticeable for AQ.

For both quinones, as HBz is added, the current for the radical anion wave grows to a two-electron value as the sec-

ond wave diminishes and shifts anodically. Figure 6A,D shows that this change depends on sweep rate in the qualitatively expected manner. The observable current function for a large excess of acid covers the entire one-to-two electron span of behavior and reflects a kinetic process within the time scale of electrochemical measurement.[11,14,47] A rough measure of the reaction velocity in Figure 6A,D can be obtained using ECE theoretical curves (first order in radical anion and in HBz). The result for DAQ for reaction half-life is 0.35 second, which is in reasonable agreement with the stop-flow homogeneous solution rate for these concentrations (first $t_{1/2}$ = 0.18 s). For AQ, the electrochemical half-life is 0.035 s, while the stopped-flow value for these concentrations is (first) $t_{1/2}$ = 0.019 s. These comparisons do indicate the absence of any gross surface catalysis of the protonation rate by mercury. The comparisons are not adequately rigorous, however, to confirm the precise protonation mechanism for the electrochemical data.

Acknowledgment. Assistance in this research was provided by the Air Force Office of Scientific Research under Grant AFOSR-73-2419 and the National Science Foundation under Grants GP38633X and GP30668. Technical assistance from Dr. R. Spell, J. Hornickel, and W. Howland is gratefully acknowledged.

References and Notes

(1) (a) University of North Carolina; (b) Davidson College.
(2) (a) R. N. Adams, "Electrochemistry at Solid Electrodes", Marcel Dekker, New York N.Y., 1969. (b) M. M. Baizer, "Organic Electrochemistry", Marcel Dekker, New York, N.Y., 1973.
(3) R. N. Adams, *Acc. Chem. Res.*, **2**, 175 (1969).
(4) G. J. Hoijtink, J. van Schooten, E. deBoer, and W. I. J. Aalbersberg, *Recl. Trav. Chim.*, **73**, 355 (1954).
(5) G. J. Hoijtink and J. van Schooten, *Recl. Trav. Chim.*, **71**, 1089 (1952).
(6) P. H. Given and M. E. Peover, *J. Chem. Soc.*, 385 (1960).
(7) M. E. Peover, *J. Chem. Soc.*, 4541 (1962).
(8) M. E. Peover, *Electroanal. Chem.*, **2**, 1 (1967).
(9) M. D. Hawley and S. W. Feldberg, *J. Phys. Chem.*, **70**, 3459 (1966).
(10) S. W. Feldberg, *J. Phys. Chem.*, **75**, 2377 (1971).
(11) L. Nadjo and J. M. Saveant, *J. Electroanal. Chem.*, **33**, 419 (1971).
(12) T. H. Ridgway, Ph.D. Dissertation, University of North Carolina, Chapel Hill, N.C., 1970.
(13) S. Feldberg, *J. Phys. Chem.*, **73**, 1238 (1969).
(14) M. Mastragostino, L. Nadjo, and J. M. Saveant, *Electrochim Acta*, **13**, 721 (1968).
(15) S. Bank and B. Bockrath, *J. Am. Chem. Soc.*, **93**, 430 (1971).
(16) D. E. Paul, D. Lipkin and S. I. Weissman, *J. Am. Chem. Soc.*, **78**, 119 (1956).
(17) G. Levin, C. Sutphen, and M. Szwarc, *J. Am. Chem. Soc.*, **94**, 2652 (1972).
(18) S. Bank and B. Bockrath, *J. Am. Chem. Soc.*, **94**, 6076 (1972).
(19) A. Rainis, R. Tung, and M. Szwarc, *J. Am. Chem. Soc.*, **95**, 659 (1973).
(20) E. R. Minnich, L. D. Long, C. M. Ceraso, and J. L. Dye, *J. Am. Chem. Soc.*, **95**, 1061 (1973).
(21) M. Petek, T. E. Neal, R. L. McNeely, and R. W. Murray, *Anal. Chem.*, **45**, 32 (1973).
(22) M. Fujihara, H. Suzuki, and S. Hayano, *J. Electroanal. Chem.*, **33**, 393 (1971).
(23) P. J. Kuduka and R. S. Nicholson, *Anal. Chem.*, **44**, 1786 (1972).
(24) R. W. Murray, W. R. Heineman, and G. W. O'Dom, *Anal. Chem.*, **39**, 1666 (1967).
(25) W. R. Heineman, J. N. Burnett, and R. W. Murray, *Anal. Chem.*, **40**, 1974 (1968).
(26) T. E. Neal, Ph.D. Dissertation, University of North Carolina, Chapel Hill, 1969.
(27) R. M. Wightman, Ph.D. Dissertation, University of North Carolina, Chapel Hill, 1974.
(28) G. Dulz and N. Sutin, *Inorg. Chem.*, **2**, 917 (1963).
(29) J. W. Strojek, G. A. Gruver, and T. Kuwana, *Anal. Chem.*, **41**, 481 (1969).
(30) R. M. Wightman, R. L. Scott, C. N. Reilley, R. W. Murray, and J. N. Burnett, *Anal. Chem.*, **46**, 1492 (1974).
(31) C. Capellos and B. H. J. Bielski, "Kinetic Systems", Wiley-Interscience, New York, N.Y., 1972.
(32) J. L. Dye and V. A. Nicely, *J. Chem. Educ.*, **48**, 443 (1971).
(33) N. C. Peterson, "Spectroscopy and Kinetics", J. S. Mattson, H. B. Mark, and M. C. McDonald, Jr., Ed., Marcel Dekker, New York, N.Y., 1973, Chapter 6.
(34) R. Jones and T. McL. Spottswood, *Aust. J. Chem.*, **15**, 492 (1962).
(35) T. Osa and T. Kuwana, *J. Electroanal. Chem.*, **22**, 389 (1969).
(36) S. Hayano and M. Fujihara, *Bull. Chem. Soc. Jpn.*, **44**, 1496 (1971).
(37) G. Vincow and G. K. Fraenkel, *J. Chem. Phys.*, **34**, 1333 (1961).
(38) J. Gendell, W. R. Miller, and G. N. Fraenkel, *J. Am. Chem. Soc.*, **91**, 4369 (1969).
(39) I. M. Kolthoff, M. K. Chantooni, and H. Smagowski, *Anal. Chem.*, **42**, 1622 (1970).
(40) I. Piljac and R. W. Murray, *J. Electrochem. Soc.*, **118**, 1758 (1971).
(41) C. D. Ritchie, "Solute-Solvent Interaction", J. F. Coetzee and C. D. Ritchie, Ed., Marcel Dekker, New York, N.Y., 1969, p. 224.
(42) B. F. Wong and N. Hirota, *J. Am. Chem. Soc.*, **94**, 4419 (1972).
(43) K. S. Chen and N. Hirota, *J. Am. Chem. Soc.*, **94**, 5550 (1972).
(44) K. Nakamura, B. F. Wong, and N. Hirota, *J. Am. Chem. Soc.*, **95**, 6919 (1973).
(45) G. R. Stevenson and L. Echegoyan, *J. Am. Chem. Soc.*, **96**, 3381 (1974).
(46) T. Kitaguwa, T. Layoff, and R. N. Adams, *Anal. Chem.*, **36**, 295 (1964).
(47) R. S. Nicholson and I. Shain, *Anal. Chem.*, **37**, 178 (1965).